An Experimental Study on Turbulent Characteristics of an Impinging Split-Triplet Injector

Shin-Jae Kang*, Ki-Wahn Ryu
Faculty of Mechanical Engineering, Chonbuk National University
Ki-Chul Kwon, Bhum-Keun Song
Graduate School, Chonbuk National University

This paper presents turbulent characteristics of an impinging F-O-O-F type injector in which fuel and oxidizer impinge on each other to atomize under the different momentum ratio. Water was used as an inert simulant liquid instead of fuel and oxidizer. The droplet size and velocity in the impinging spray flow field were measured using a PDPA. The gradient of the spray half-width(b_2) along the long-axis direction declined throughout the entire spray flow field with increasing the momentum ratio from 1.19 to 6.48. However, the gradient of the half-width(b_1) along the short-axis direction decreased with increasing the momentum ratio. The turbulence intensity and turbulent kinetic energy were converged into the center of the initial region with increasing the momentum ratio. As the momentum ratio increased from MR=1.19 to MR=6.48, the turbulent shear stress decreased. The results of this study can be used for the design of an impinging type injector for liquid rockets.

Key Words : Impinging Injector, Phase Doppler Particle Anayzer(PDPA), Momentum Ratio(MR), Half-Width, Turbulence Intensity, Turbulent Kinetic Energy, Turbulent Shear Stress

Nomenclature

- b_1 : Spray half-width along the short-axis direction
- b_2 : Spray half-width along the long-axis direction
- b_0 : Mean value of b2/b1
- Xo : Imaginary impinging distance of fuel jet [15.59 mm]
- Ti : Turbulence intensity
- Ke : Turbulent kinetic energy
- $\overline{u'v'}$: Turbulent shear stress
- r : Mixture ratio
- MR : Momentum ratio

* Corresponding Author,
E-mail : sjkang@jnplab.chonbuk.ac.kr
TEL : +82-63-270-2387 ; **FAX** : +82-63-270-2472
Faculty of Mechanical Engineering, Chonbuk National University, Automobile High Technology Research Institute, 664-14, Dukjin-dong, Dukjin-gu, Chonju, Chonbuk 561-756, Korea. (Manuscript **Received** May 22, 2000; **Revised** October 9, 2000)

1. Introduction

A liquid rocket engine which is employed widely in a space system has been investigated over the half century. The ability to provide complete atomization of the liquid propellant is essential to the development of liquid rocket engines possessing high combustion efficiencies and performance characteristics. Hence, considerable attention is being concentrated on the injector which significantly affects the combustion stability and atomization.

In this study, an impinging type injector, which is used in the middle · low thrust rocket system, was investigated. This injector produces particles by impingement between the fuel and oxidizer jets.

The impinging injector can be classified into two types, namely the liquid/liquid and the liquid/gas. These types are also classified into the

Like-impinging type, in which fuel impinges on fuel and oxidizer impinges on oxidizer, and the Unlike-impinging type, in which fuel impinges on oxidizer. There are several types of injectors by impinging form and number of orifices. A doublelet Oxidizer-Fuel(O-F) type injector has one oxidizer orifice and one fuel orifice, in which the oxidizer and fuel jets impinge on each other. A triplet O-F-O(F-O-F) type injector is that two oxidizer(fuel) jets from the outside orifices impinge on the fuel(oxidizer) jet from the center orifice. A double impinging F-O-O-F type injector is that the fuel jets through outer orifices initially impinges on the oxidizer jets from center orifices, and then these impinged jets impinge again to form the sprays. A quardlet type injector has one fuel orifice in the middle and three oxidizer orifices outside at an interval of 120°.

Fuel and oxidizer are mixed and atomized by the impinging momentum in the impinging type injector. Therefore, the impinging type is comparatively simple and economical, and it also does not need high pressure. For these reasons, the impinging type injector is used considerably in liquid rocket engines. The atomization characteristics and mixing efficiencies of the impinging type injector were analyzed by Rupe(1956), Elverum-Morey(1959), Ferrenberg(1985) and Kuykendal et al. (1970). Furthermore, Kim(1996) and Kang et al. (2000) studied the effect of the pressure drop, impinging angle and momentum ratio of the propellant on the spray characteristics.

Another significant factor that influences the real combustion efficiencies is the turbulent characteristics. In the process of combustion, heat and material transfer is occurred rapidly. Hence, it is evident that the turbulence characteristics of flow field govern the spray behaviour. Rho et al. (1998) investigated the turbulent shear stress with the swirl angle in a two-phase swirling jet. Kim. (1987) and Rho et al. (1990) analyzed the air-air impinging jet formed by the impingement of the round jet. However, many researches for the liquid-liquid impinging jet have not been carried out until now.

The purpose of this paper is to investigate the spray half-width, turbulence intensity, turbulent kinetic energy and turbulent shear stress of F-O-O-F type impinging injector using a PDPA system. Water was used in lieu of fuel and oxidizer.

2. Test Facilities and Experimental Arrangement

The test facilities to investigate the atomization characteristics of impinging injectors are composed of a simulant propellant feeding system, an injector and a laser measurement system.

The propellant feeding system delivers the propellant from the propellant tank to the injector. An industrial displacement pump was employed to supply the propellant continuously to the injector at high pressure and flow rate. This pump can provide a maximum discharge flow rate of 99 ℓ/min and a maximum discharge pressure of 60 kgf/cm^2. In addition, a ball valve, which can resist high pressures, was used to control the flow rate. The suppling pressure was measured just before the simulant propellant was provided to the injector.

The injector is an F-O-O-F type in which the outward two fuel jets impinge on the inward two oxidizer jets to mix and atomize the propellant.

The specification of the uni-element injector applied in this study is shown in Fig. 1 and Table 1. Fuel is injected through the Orifices ① and ④ and oxidizer through the Orifices ② and ③. The fuel stream through Orifice ① initially impinges on the oxidizer stream from ② (③ impinges on ④). These initially impinged jets impinge again and then form the spray.

A three dimensional phase Doppler particle analyzer (PDPA) was employed to measure the atomized droplet size and velocity components. A schematic diagram of PDPA system is shown in Fig. 2. The PDPA consists of an optical system, a signal processing system and a three dimensional traversing system. The optical system is composed of transmitting & receiving optics, and a 350mW air-cooled Ar-ion laser was used. Transmitting optics make three different laser beams cross at the measurement point. Receiving optics detect the scattered light, which is produced when the droplets pass through the measurement volume,

Table 1 Design values of Injector

Type	F-O-O-F
First impinging angle(θ_1)	30°
First impinging length(L_1)	10.39 mm
Oxidizer orifice diameter	2.2 mm
Fuel orifice diameter	1.6 mm

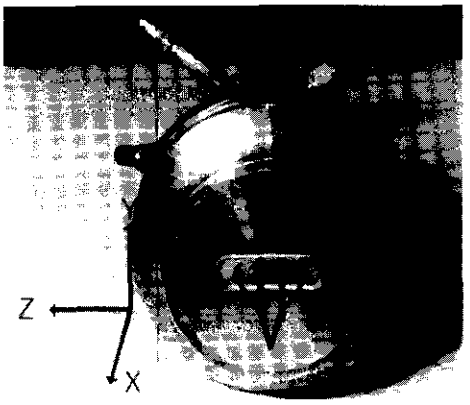

Fig. 1 Figure of F-O-O-F type injector.

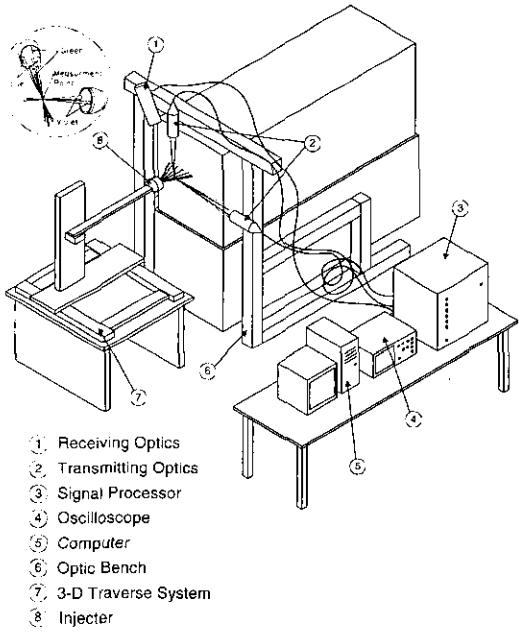

Fig. 2 Schematic diagram of PDPA System

and then transmit it to the signal processor. The signal processor (DANTEC model 58N50) is a burst detector type. Therefore, the size and velocity are measured by frequency and relative phase

Table 2 Spary conditions

(Unit $\dot{m}$: g/s, P : kPa)

r	MR	$\dot{m}_f$	$\dot{m}_o$	P_f	P_o
1.50	1.19	104.0	156.0	725.3	532.5
2.00	2.12	86.70	173.3	503.5	657.7
2.47	3.22	75.00	185.0	377.1	749.5
3.00	4.76	65.00	195.0	283.2	832.2
3.50	6.48	57.80	202.2	223.8	895.0

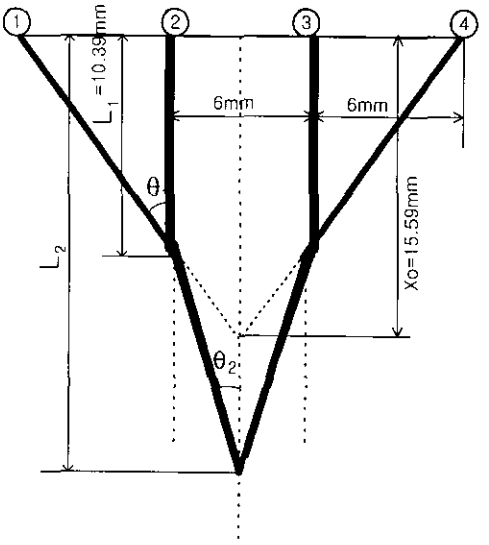

Fig. 3 Impinging angle and length of F-O-O-F type injector

difference of the Doppler signal. The voltage provided to a receiving optic sensor was fixed at 1400 V. At each measuring point, 10,000 droplets were sampled and sampling time was limited to within 10 seconds.

Atomized droplet size and velocity were measured for various oxidizer/fuel ratios. The total flow rate was fixed at 260 g/s. A change of a momentum ratio(Eq. (1)) means a change in the mixture ratio ($r=\dot{m}_o/\dot{m}_f$).

$$\text{Momentum Ratio(MR)}=\frac{\dot{m}_o v_o}{\dot{m}_f v_f}$$

$$=\left(\frac{\dot{m}_o}{\dot{m}_f}\right)^2\frac{\rho_f A_f}{\rho_o A_o}=\left(\frac{\dot{m}_o}{\dot{m}_f}\right)^2\frac{\rho_f}{\rho_o}\left(\frac{d_f}{d_o}\right)^2 \quad (1)$$

Table 2 shows the experimental conditions. In the F-O-O-F type injector, the impinging angle

Table 3 Second impinging angle and length

r	MR	Second impinging angle(θ_2)	Second impinging length(L_2)
1.50	1.19	13.67°	22.72 mm
2.00	2.12	10.66°	26.32 mm
2.47	3.22	7.65°	32.74 mm
3.00	4.76	5.45°	41.84 mm
3.50	6.48	4.11°	52.12 mm

and length affect the spray characteristics significantly due to the secondary impingement. The impinging forms and the theoretical impinging angle and length are shown in Fig. 3 and Table 3.

3. Results and Discussion

3.1 Spray half-width

The axial mean velocity has been normalized with the maximum mean velocity, $\bar{U}_m$, and Xo has been used to define a normalized flow direction. Xo is the imaginary cross point with respect to fuel jets, and can be defined as Xo=15.59 mm. Figure 4 shows longitudinal development of the half-widths along the Y and Z axes, which are perpendicular to the flow.

The gradient of the spray half-width(b_2) along the long-axis direction(Y) declined with increasing the momentum ratio from 1.19 to 6.48. This is mainly attributed to the momentum decrease of the outer jets. Similarly, the gradient of the half-width(b_1) along the short-axis direction(Z) decreased with increasing the momentum ratio. Rho et al. (1990) reported the work on the flow field of the air-cross jet that the half-width(b_1) of the cross section along the short-axis direction was contracted after collision of the jets, in the initial region where the inertia force to keep moving to the Z-axis direction with the half of the impinging angle influenced strongly, but it was elongated with being far from the initial region. Moreover, the half-width(b_2) along the long-axis plane in the initial region was elongated as much as the width along the short-axis plane was contracted. However, the half-width(b_2) elongation along the long-axis was reduced gradually with being far

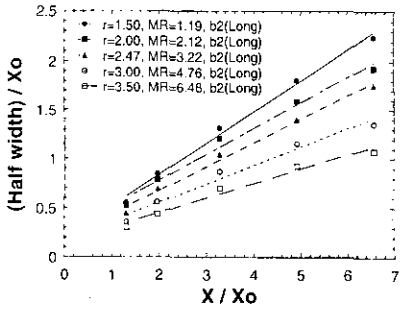

(a) Half width of long axis(b_2)

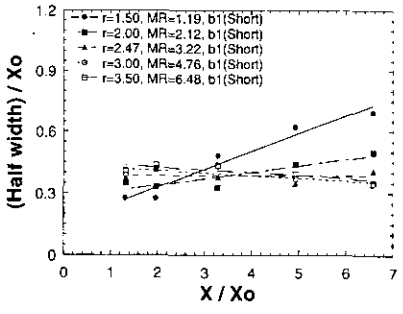

(b) Half width of short axis(b_1)

Fig. 4 Variation of half width along the centerline with different momentum ratios

from the initial region, because the effect of the inertia force was vanished. Hence, Rho et al. (1990) divided air-cross jet flows in two region, the large and small elongation region. However, in this liquid-liquid impinging study, the results were a bit different from those of Rho et al. (1990). There was no point that the difference in the gradient was remarkable so as to divide the spray regions into the large and small elongation regions.

According to Rho et al. (1990), there was the region where the spray half-width(b_1) along the short-axis direction(Z) was contracted after impingement. The contraction region, however, could not be examined in this study. The measurement should be performed in many points after impingement in order to investigate the contraction region. In case of the liquid-liquid impingement, however, the measurement could not be performed in the fore part that the impinged jet was not break up into droplets. Subsequently, the contraction region after impingement could not be investigated.

The spray half-width(b_2) along the long-axis direction increased with going up the axial distance, but it decreased with increasing the momentum ratio due to the decrease of the momentum of the fuel jets. The spray half-width(b_1) along the short-axis direction at MR= 1.19 and 2.12 decreased with going up the axial distance in the initial region, but it increased with being far from the initial region. In contrast, the half-width(b_1) along the short-axis direction at MR=3.22, 4.76 and 6.48 increased in the initial region, but it declined with being far from the initial region. In case of the low momentum ratio, the momentum of the fuel jets was high and the momentum of the oxidizer jets was low, the spray half-width(b_1) was contracted in the initial region due to the high momentum of the fuel jets to keep moving to the Z-direction with 30 degree after impingement, but it was elongated with being far from the initial region due to the repulsion of fuel jets. In case of the high momentum ratio, the fuel jets could not split the oxidizer jets, and thus, it was forced out of the spray. As a result, the spray half-width(b_1) was elongated in the initial region, but it was contracted in other region.

Figure 5 indicates the results of this study at MR=1.19 comparing with Rho et al. (1990). Where the Reynolds number was 5.2×10^4. The spray half-width(b_2) along the long-axis distance(Y) in the liquid-liquid impingement flow was larger than in the air-air impingement flow, and the elongation rate did not decrease significantly, as shown in Fig. 5. It is assumed that this phenomenon occurred because a decrease in the inertia force occurred faster for the air-air impingement, decreasing rate is also higher than for the liquid-liquid impingement, and the air-air impingement flow disperses to the ambient air at a much higher rate than the liquid-liquid impingement flow. The elongation rate of the spray half-width(b_1) along the short-axis distance(Z) was higher for the air-air impingement flow. This is because the diffusion to the surroundings was superior the case of the air-air impingement to the case of the liquid-liquid impingement, which was occurred by low density and viscosity.

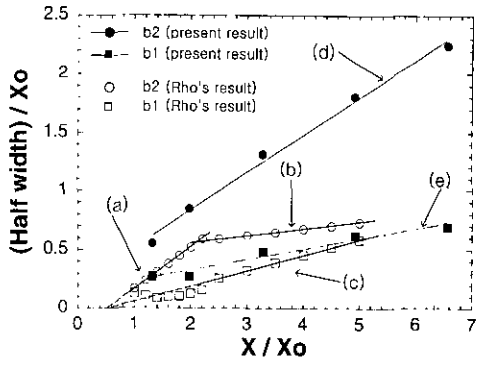

Fig. 5 Comparison of half width between the Rho's result with an air-cross jet and the present result with a liquid-cross jet.
((a) $b_2/X_o=-0.18+0.35(X/X_o)$,
(b) $b_2/X_o=0.45+0.056(X/X_o)$,
(c) $b_1/X_o=-0.067+0.13(X/X_o)$,
(d) $b_2/X_o=0.2015+0.3285(X/X_o)$,
(e) $b_1/X_o=0.1526+0.0877(X/X_o)$)

3.2 Turbulence intensity, turbulent kinetic energy, turbulent shear stress

The factor to determine the feature of the combustion field is the velocity distribution of the flow field in the liquid fuel or gas fuel combustion. The factor to determine the characteristics of the combustion field and products after combustion is the distribution feature of turbulent components in the flow field. In general, the turbulence results from the shear stress by the gradient of velocities in the flow field and the small scale of material transfer in the shear layer. Accordingly, turbulent characteristics of the flow field determine the flow behaviour in the phenomenon that heat and materials are remarkably transferred such as combustion.

The magnitude of the turbulent shear stress as the turbulent characteristic value produced by the gradient of velocities increases with augmenting the velocity differences between fluid shear layers. The measured value of the turbulent shear stress, however, is rarely used in application parts. Nevertheless, the reason why the turbulent shear stress is the significant factor of the turbulent flow characteristics is that it is difficult to process when the turbulence is theoretically expressed.

In general, when the physical phenomena are

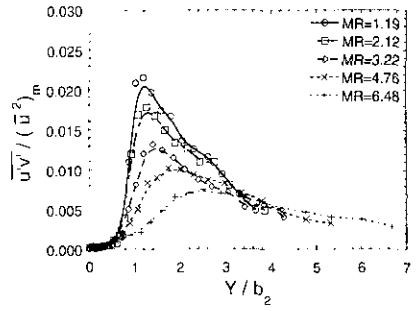

(a) X=30 mm, Y-direction

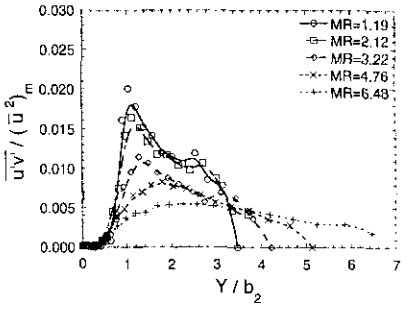

(b) X=50 mm, Y-direction

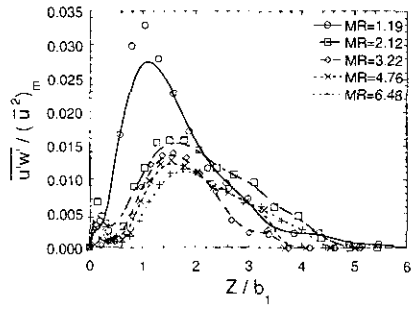

(c) X=30 mm, Z-direction

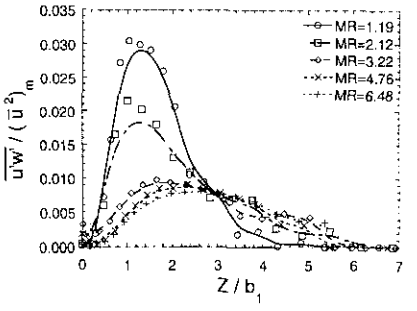

(d) X=50mm, Z-direction

Fig. 6 Distributions of the turbulent sheart stress

simplified and modelled so as to analyze with ease, the use of the measured value of the turbulent shear stress improves the accuracy of the results obtained by theoretical approach.

Figure 6 indicates the turbulent shear stress with the different momentum ratio at X=30 and 50 mm. From the figure, it shows that the turbulent shear stress is low with increasing the momentum ratio. This trend occurs because the waving velocity components along both Y and Z directions, v' and w', are reduced by the momentum increase of the oxidizer jets and the momentum decrease of the fuel jets with increasing the momentum ratio.

In Fig. 6, the magnitude of the turbulent shear stress($\overline{u'w'}/\overline{u}^2_m$) above MR=3.22 was nearly the same. This is mainly because the flow pattern of the impinging jet is changed into the flow pattern of the free circular jet by not only the momentum increase of the oxidizer jets but the momentum decrease of the fuel jets.

The turbulence intensity and turbulent kinetic energy are defined as Eq. (2) and (3) in the three dimensional flow field.

$$Ti=\frac{\sqrt{\frac{\overline{u'^2}+\overline{v'^2}+\overline{w'^2}}{3}}}{\overline{u}_m} \tag{2}$$

$$Ke=\frac{1}{2\overline{u}_m^2}(\overline{u'^2}+\overline{v'^2}+\overline{w'^2}) \tag{3}$$

The turbulence intensity at MR=2.12 and 6.48 is illustrated in Fig. 7. For MR=2.12, the turbulence intensity in the X-Y plane is distributed strongly in the location which is 20 mm~30 mm away from the axial centerline. The turbulence intensity along the X-Z plane is extremely high in 10 mm~20 mm away from the axial centerline. For MR=6.48, the strong turbulence intensity along the X-Y plane is converged into the center of the initial region. It can be observed from Fig. 8 that the trend of the turbulent kinetic energy distributions is similar to the turbulence intensity distributions. In case of the high momentum ratio, MR=6.48, the momentum of the fuel jets is low and the momentum of the oxidizer jets is high. So, the fuel jets cannot break up the oxidizer jets, and thus, the fuel jets is forced out of the oxidizer jets. As a result, the oxidizer exists in center of spray,

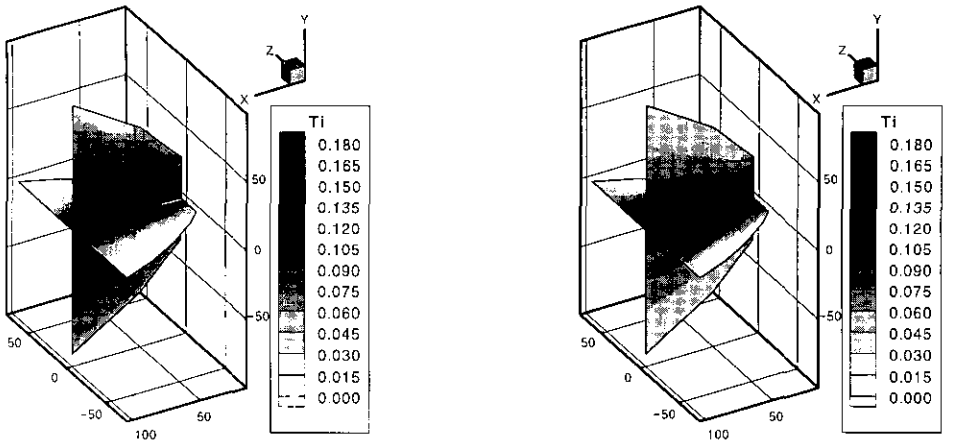

(a) r=2.00, MR=2.12 (b) r=3.50, MR=6.48

Fig. 7 Distributions of turbulent intensity

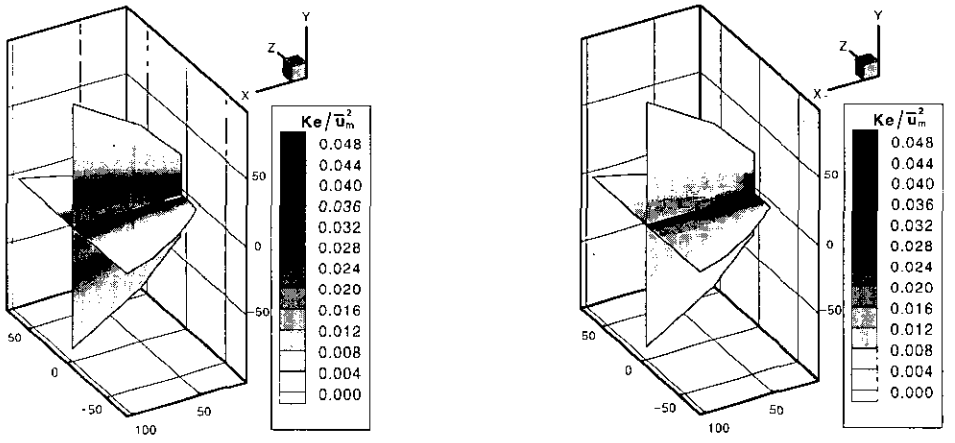

(a) r=2.00, MR=2.12 (b) r=3.50, MR=6.48

Fig. 8 Distributions of turbulent kinetic energy

and the fuel exists in outside of spray. This means that the fuel and oxidizer is not mixed well each other.

The magnitude of the turbulence intensity along the X-Z plane is high as shown in Fig. 7. Because the velocity is changed very rapidly in a narrow region (see Fig. 9). It is convinced from Fig. 9 which shows the one dimensional turbulence intensity at MR=2.12 and X=100 mm that the turbulence intensity is high near the center of the Z-axis, but it is low near the center of the Y-axis.

From these results, the mixing of fuel and oxidizer will be improved, when the turbulence intensity and turbulent kinetic energy are not

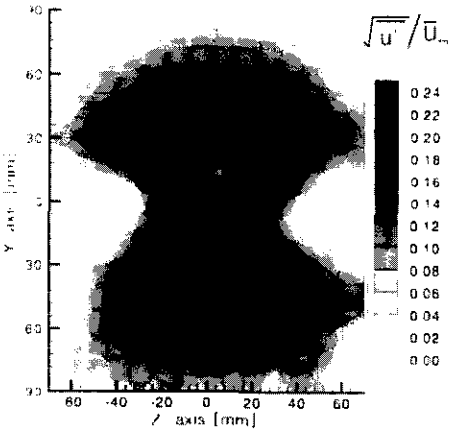

Fig. 9 Distribution of 1-D turbulent intensity (Y-Z plane, X=100mm)

converged into the initial region and the strong turbulent characteristics appear in the whole region of spray.

4. Conclusions

From the analysis of the turbulent characteristics of a double impinging F-O-O-F type injector for liquid rockets, some significant factors can be summarized as follows.

(1) The gradient of the spray half-width(b_2) along the long-axis direction(Y) declined with increasing the momentum ratio from 1.19 to 6.48. This is mainly attributed to the momentum decrease of the outer jets. Similarly, the gradient of the half-width(b_1) along the short-axis direction(Z) decreased with increasing the momentum ratio.

(2) The turbulent shear stress is low with increasing the momentum ratio, and the form of its distributions for the momentum ratio above 3.22 was similar to the flow pattern of a free round jet. This trend is occurred because the waving velocity components along both Y and Z directions, v' and w', are reduced by momentum increase of the oxidizer jets and momentum decrease of the fuel jets with increasing the momentum ratio.

(3) In case of the low momentum ratio, MR=2.12, the strong turbulence intensity and turbulent kinetic energy along the X-Y plane appear in the region which is 20 mm~30 mm away from the axial centerline. In addition, the strong turbulence intensity and turbulent kinetic energy along the X-Z plane appear in the region which is 10 mm~20 mm away from the axial centerline. In case of the high momentum ratio, MR=6.48, the strong turbulence intensity and kinetic energy along the X-Y and X-Z plane are converged into the center of the initial region.

References

Elverum, G. W., and Morey, T. F., 1959, *Criteria for Optimum Mixture Ratio Distribution Using Several Types of Impinging Stream Injector Elements,* Memorandum No. 30-5, Jet Propulsion Laboratory, California Institute of Technology, Pasadena, California.

Ferrenberg A., and Jaqua, V., 1985, *Atomization and Mixing Study,* Contract Nas 8-34504, Rocketdyne Report No. RI/RD85-312.

Kang, S. J., Rho, B. J., Oh, J. H. and Kwon, K. C., 2000, "Atomization Characteristics of a Double Impinging F-O-O-F Type Injector with Four Streams for Liquid Rocket," *KSME International Journal*, Vol. 14, No. 4, pp. 466~476.

Kim, Y., Jeong, H. S., Kim, S. J., and Park S. W., 1994, "A Study on Spray Characteristics with Design Variables of Impinging Type Doublet Injector," *Journal of KSAS*, Vol. 22, No. 6, pp. 8~14.

Kuykendal, W. B., 1970, *The Effects of Injector Design Variables On Average Drop Size for Impinging Jets,* AFRPL-TR-70-53.

Park, S. Y., Kim, S. J., Park, S. W., and Kim, Y., 1996, "A Study on Spray Characteristics of the Triplet Impinging Stream Type Injector for Liquid Rocket," *Transactions of KSME*, Vol. 20, No. 3, pp. 1005~1014.

Rho, B. J., Kang, S. J., Choi, J. C., and Oh, J. H., 1990, "An Experimental Analysis of the Mixing Flow Field of a Turbulent Cross Jet," *Proceedings of The Second KSME-JSME Fluids Engineering Conference*, Vol. 1, pp. 119~124.

Rho, B. J., Kang, S. J., Oh., and Lee, S. G., 1998, "Swirl Effect on the Spray Characteristics of a Twin-Fluid Jet," *KSME International Journal*, Vol. 12, No. 5, pp. 899~906.

Rho, B. J., Kim, J. K., and Dwyer, H. A., 1990, "Experimental Study of a Cross Jet," *AIAA Journal*, Vol. 28, No. 5, pp. 784~789.

Rho, B. J., Oh, J. H., and Han, I. K., "An Experimental Study on the Mixing Flow Structure of a 45° Cross Jet with Velocity Variation," *Journal of KSAS*, Vol. 21, No. 6, pp. 56~67.

Rupe, J. H., 1956, *A Correlation Between the Dynamic Properties of a Pair Impinging Streams and the Uniformity of Mixture Ratio Distribution in the Resulting Spray,* Jet Propulsion Laboratory, California Institute of Technology, Pasadena, California.